Supporting Information

Song et al. 10.1073/pnas.1218581109

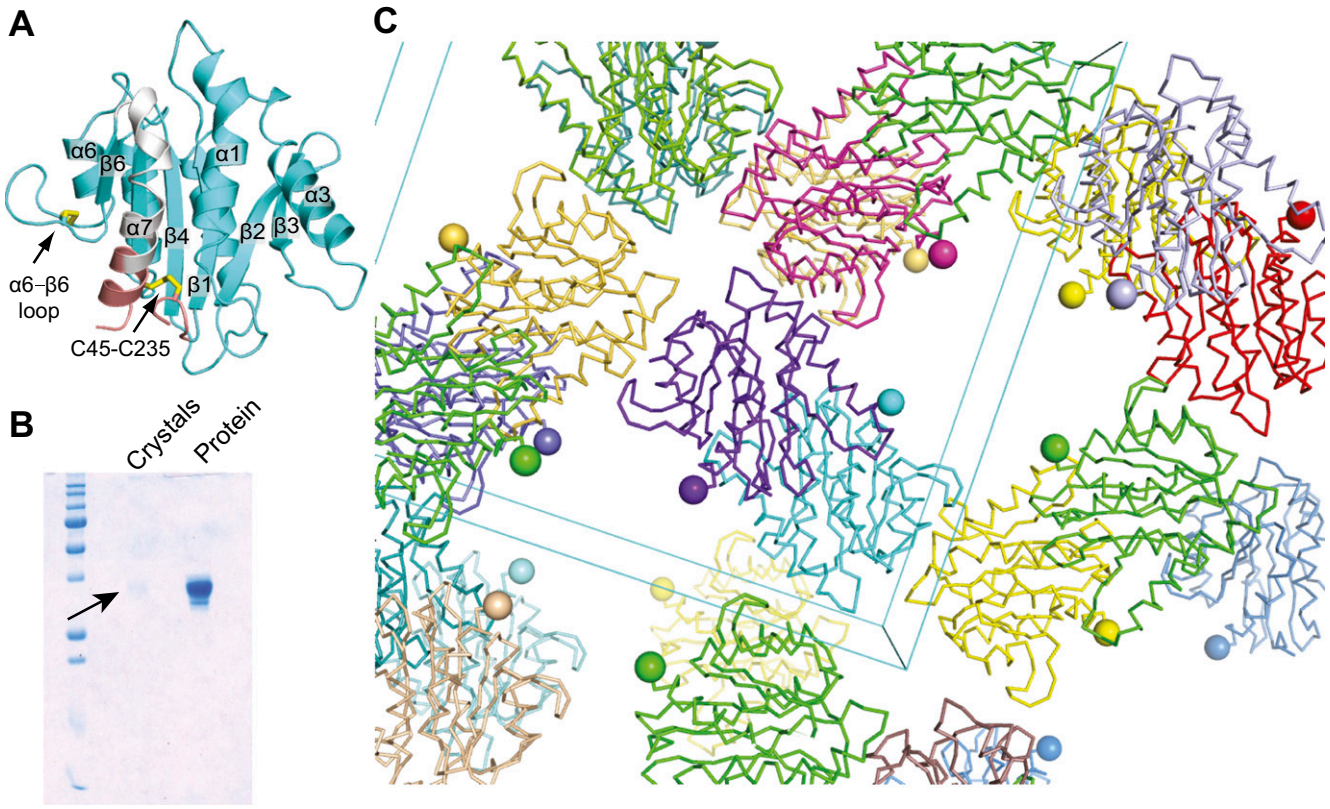

Fig. S1. TSR domain is present in pfTRAP (26-299) crystals, but missing in electron density. (*A*) The structure of pfTRAP (26–299) VWA domain in the same orientation as in Fig. 1 *B* and *C*. (*B*) SDS/PAGE of dissolved crystals and the TRAP protein that was subjected to crystallization. (*C*) Packing of pfTRAP (26–299) VWA domain in crystal lattice. The chains are shown as ribbons and the Cα of terminal residues K240 are shown as spheres.

```
                E-βA        β1                α1                      β2       β3
pvTRAP  DEKVVDEVKYSEEVCNESVDLYLLVDGSGSIGYPNWITKVIPMLNGLINSLSLSRDTINLYMNLFGNYTTELIRL   99
PfTRAP  QNNIVDEIKYREevcnDEVDLYLLMDGSGSIRRHNWVNHAVPLAMKLIQQLNLNDNAIHLYASVFSNNAREIIRL  103
MIC2    DVIQSDSAIGAAEGctNQLDICFLIDSSGSI-GIQNFRLVKQFLHTFLMVLPIGPEEVNNAVVTYSTDVHLQWDL  136
                     ↑
CMG2    ------------scrRAFDLYFVLDKSGSV-AN-NWIEIYNFVQQLAERFVSP--EMRLSFIVFSSQATIILPL   95
Mac1    -----------------DSDIAFLIDGSGSI-IPHDFRRMKEFVSTVMEQLKKS--KTLFSLMQYSEEFRIHFTF  186
VWFA3   --------------csQPLDVILLLDGSSSF-PASYFDEMKSFAKAFISKANIGPRLTQVSVLQYGSITTIDVPW 1745
          α2       α3                    α4                    β4            α5
pvTRAP  GSGQSIDKRQALSKVTELRKTYTPYGTTNMTAALDEVQKHLNDRVN--REKAIQLVILMTDGVPN--SKYRALEV  170
pfTRAP  HSDASKNKEKALIIIKSLLSTNLPYGKTSLTDALLQVRKHLNDRIN--RENANQLVVILTDGIPD--SIQDSLKE  174
MIC2    QSPNAVDKQLAAHAVLDM---PYKKGSTNTSDGLKACKQILFTGsrpgREHVPKLVIGMTDgesd--sdfrtvRA  200
CMG2    T----GDRGKISKGLEDLkR-VSPVGETYIHEGLKLANEQIQKa--gg-lkTSSIIIALTDGKLDglvpsyAEKE  162
Mac1    K-efqn-nPNPRSLVKPI---TQLLGRTHTATGIRKVVRELFNItngaRKNAFKILVVITDGEKFg-dplgYEDV  255
VWFA3   N-vv-pEKAHLLSLVDVM---QREGGPSQIGDALGFAVRYLTSemhgaRPGASKAVVILVTDVSV----dsVDAA 1811
                 β5              α6                  β6       α7
pvTRAP  ANKLKQRNVSLAVIGIGQGI----NHQFNRLIAGCRPR---EPNCKFYSYA--DWNEAVALI--KPFIAKVCTE   233
PfTRAP  SRKLSDRGVKIAVFGIGQGI----NVAFNRFLVGCHPS---DGKCNLYADS--AWENVKNVI--GPFMKAVCVE   237
MIC2    AKEIRELGGIVTVLAVGHYV----KHSECRSMCGCSGTSDDDSPCPLYLRA--DWGQLATAI--KPMLKEVCKT   266
CMG2    AKISRSLGASVYCVGVLD-F----EQAQLERIADsk---------EQVFPVkggFQALKGII--NSILAqsc--   218
Mac1    IPEADREGVIRYVIGVGDAFrsekSRQELNTIASkpp-------rDHVFQVn-NFEALKTIQ--NQLREKIFA-   318
VWFA3   ADAARSNRVTVFPIGIGDRY----DAAQLRILAGpag-------dSNVVKlqRIEDLPTMVtlgNSFLHKLc--  1872
         E-βB      TSR-1      TSR-β2                                TSR-β3
pvTRAP  VERVANCGPWDPWTACSVTCGRGTHSRSRPSLH----------------EKCTTH----MVSECEEGECP     283
pfTRAP  VEKTASCGVWDEWSPCSVTCGKGTRSRKREILH----------------EGCTSE----LQEQCEEERCL     287
MIC2    LPQDAICSDWSAWSPCSVSCGDGSQIRTRTEVSAPQPGTPTCPDCPAPMGRTCVEQGGLEEIRECSAGVCA     337
```

Fig. S2. Structure-based alignment of TRAP with representative VWA domains. VWA domain structures were aligned using secondary-structure matching (1). Some gaps were closed up manually; resulting structurally nonequivalent aligned residues are in lowercase. Residues not present in crystallized proteins or missing in density are in italics. Aligned structures are MIC (2), CMG2 (3), Mac-1 (4), and VWF A3 (5). The MPP2 cleavage site in MIC2 is indicated by an arrow.

1. Krissinel E, Henrick K (2004) Secondary-structure matching (SSM), a new tool for fast protein structure alignment in three dimensions. *Acta Crystallogr D Biol Crystallogr* 60(Pt 12 Pt 1): 2256–2268.
2. Tonkin ML, Grujic O, Pearce M, Crawford J, Boulanger MJ (2010) Structure of the micronemal protein 2 A/I domain from Toxoplasma gondii. *Protein Sci* 19(10):1985–1990.
3. Lacy DB, Wigelsworth DJ, Scobie HM, Young JA, Collier RJ (2004) Crystal structure of the von Willebrand factor A domain of human capillary morphogenesis protein 2: An anthrax toxin receptor. *Proc Natl Acad Sci USA* 101(17):6367–6372.
4. Lee JO, Rieu P, Arnaout MA, Liddington R (1995) Crystal structure of the A domain from the α subunit of integrin CR3 (CD11b/CD18). *Cell* 80(4):631–638.
5. Bienkowska J, Cruz M, Atiemo A, Handin R, Liddington R (1997) The von willebrand factor A3 domain does not contain a metal ion-dependent adhesion site motif. *J Biol Chem* 272(40): 25162–25167.

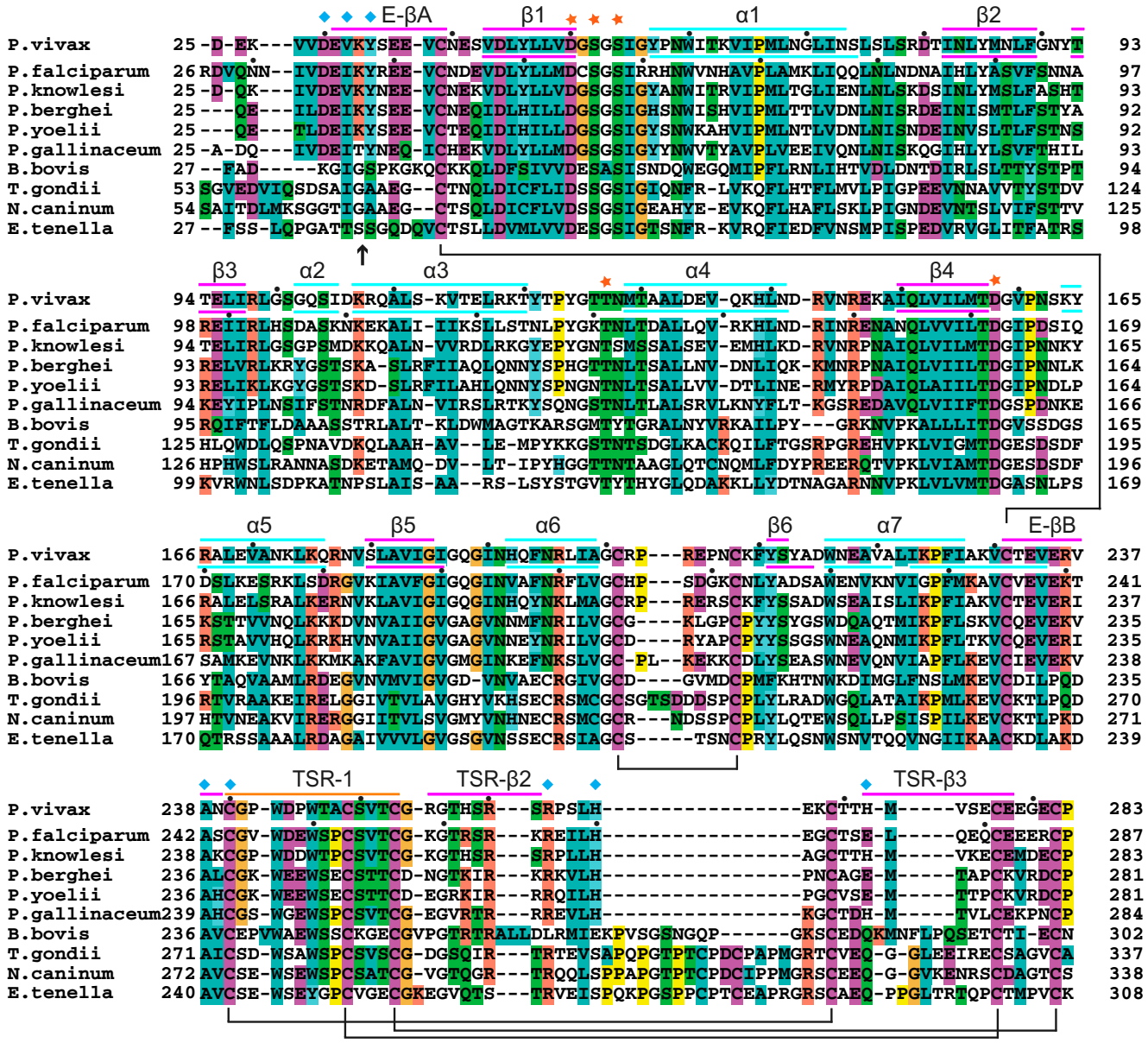

Fig. S3. Sequence alignment of the N-terminal TRAP segment containing the VWA and TSR domains with orthologs in other apicomplexan species. Sequences have GenBank accession numbers AAC97484 (*P. vivax*), AAA29775 (*P. falciparum*), AAG24613 (*Plasmodium knowlesi*), AAB63302 (*Plasmodium berghei*), AAA29768 (*Plasmodium yoelii*), AAC47461 (*Plasmodium gallinaceum*), ACM44016 (*Babesia bovis*), AAB63303 (*Toxoplasma gondii*), AAF01565 (*Neospora caninum*), and AAD03350 (*Eimeria tenella*). Secondary structures are marked above the sequences of *P. vivax* and *P. falciparum* TRAP constructs. MIDAS residues are marked with asterisks. Disulfide-bonded residues are linked by black lines for *P. vivax* and *P. falciparum*. Conserved residues within the interface between the extensible β ribbon and TSR domain are marked with blue diamonds. Black dots mark decadal residues. In MIC2, E-βA differs. The long loop between TSR-β2 and TSR-β3 in MIC2 with its additional two cysteines is predicted to extend the interaction interface between the TSR domain and extensible β ribbon and compensate for the different character of extensible β ribbon E-βA in MIC2.

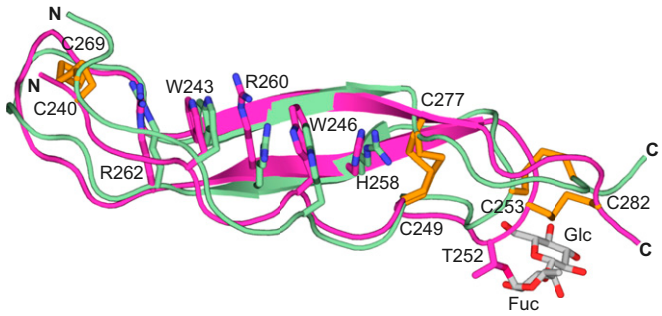

Fig. S4. Superposition of TRAP TSR domains from *P. vivax* crystal structure and *P. falciparum* NMR structures. Backbones are magenta for *P. vivax* and green for *P. falciparum* (model 1 of PDB ID 2BBX). The TSR layer residues and the carbohydrate (present only in the crystal structure) are shown as sticks. Residue numbering is for *P. vivax*; His258 is Arg in *P. falciparum*.

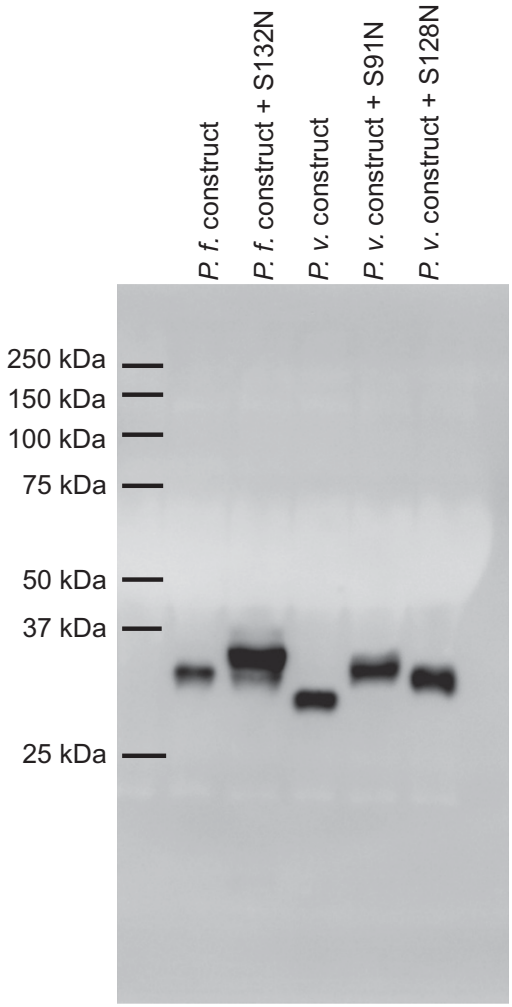

Fig. S5. *N*-glycosylation of back-mutated constructs in 293T cells. The crystallization constructs with all potential *N*-linked sites mutated and indicated back-mutations to wild-type sequence are compared. Culture supernatants from transient transfections were subjected to reducing SDS 12.5% PAGE and anti-His Western blotting.

Table S1. Data collection and refinement statistics

	pfTRAP (26-299)	pfTRAP (41-240)	pvTRAP	pvTRAP (Mg)	pvTRAP (Mn)
Data					
Space group	I4	$P42_12$	$P2_12_12_1$	$P2_12_12_1$	$P2_12_12_1$
Cell dimensions					
a, *b*, *c* (Å)	110.2, 110.2, 47.0	117.7, 117.7, 65.5	56.3, 100.5, 158.6	59.6, 98.0, 159.2	59.6, 98.6,159.5
α, β, γ (°)	90, 90, 90	90, 90, 90	90, 90, 90	90, 90, 90	90, 90, 90
Resolution (Å)	43.27–2.2 (2.26–2.2)	41.03–2.25 (2.29–2.25)	42.43–2.2 (2.24–2.2)	41.72–2.24 (2.28–2.24)	39.88–2.2 (2.24–2.2)
R_{sym}*	0.165 (1.123)	0.157 (1.000)	0.071 (0.315)	0.085 (0.353)	0.132 (0.948)
I/σI	11.26 (1.69)	10.22 (1.28)	16.72 (3.69)	13.73 (4.36)	10.61 (1.49)
Completeness (%)	98.1 (97.5)	99.9 (99.6)	98.3 (88.0)	99.6 (99.1)	99.7 (99.4)
Redundancy	2.89 (2.80)	6.8 (5.7)	3.8 (3.5)	4.0 (3.8)	4.0 (3.8)
Refinement					
Resolution (Å)	43.27–2.2	41.03–2.25	42.43–2.2	41.72–2.24	39.88–2.2
No. reflections	14,268	22,394	46,091	45,385	47,461
R_{work}/R_{free}†	0.17/0.22	0.19/0.24	0.16/0.20	0.16/0.20	0.17/0.21
rms deviations					
Bond lengths (Å)	0.008	0.003	0.009	0.008	0.007
Bond angles (°)	1.10	0.70	0.99	1.00	0.99
Residue range	41–240	41–240	25–283	28–283	28–283
Ramachandran (%)‡	98.0/2.0/0	96.7/3.3/0	96.3/3.7/0	97.4/2.6/0	96.1/3.9/0
PDB code	4HQF	4HQK	4HQO	4HQL	4HQN

Values for highest resolution shells are in parentheses.

*$R_{sym} = \Sigma i,h|I(i,h) - \langle I(h)\rangle|/\Sigma i,h|I(i,h)|$ where $I(i,h)$ and $\langle I(h)\rangle$ are the *i*th and mean measurement of intensity of reflection *h*.

†R_{free} was calculated using 5% of the data.

‡Residues in favored, accepted, and outlier regions of the Ramachandran plot as reported by MOLPROBITY.